



HAL
open science

Top-down Approach for the Direct Synthesis, Patterning, and Operation of Artificial Micromuscles on Flexible Substrates

Ali Maziz, Cedric Plesse, Caroline Soyer, Eric Cattan, Frederic Vidal

► To cite this version:

Ali Maziz, Cedric Plesse, Caroline Soyer, Eric Cattan, Frederic Vidal. Top-down Approach for the Direct Synthesis, Patterning, and Operation of Artificial Micromuscles on Flexible Substrates. ACS Applied Materials & Interfaces, Washington, D.C. : American Chemical Society, 2016, 3, pp.1559-1564. 10.1021/acsami.5b09577 . hal-02980109

HAL Id: hal-02980109

<https://hal-cyu.archives-ouvertes.fr//hal-02980109>

Submitted on 6 Jul 2022

HAL is a multi-disciplinary open access archive for the deposit and dissemination of scientific research documents, whether they are published or not. The documents may come from teaching and research institutions in France or abroad, or from public or private research centers.

L'archive ouverte pluridisciplinaire **HAL**, est destinée au dépôt et à la diffusion de documents scientifiques de niveau recherche, publiés ou non, émanant des établissements d'enseignement et de recherche français ou étrangers, des laboratoires publics ou privés.



Distributed under a Creative Commons Attribution - NonCommercial | 4.0 International License

Top-down Approach for the Direct Synthesis, Patterning, and Operation of Artificial Micromuscles on Flexible Substrates

Ali Maziz,¹ Cédric Plesse,¹ Caroline Soyer,[#] Eric Cattan,^{*,#} and Frédéric Vidal¹

¹LPPI, EA2528, Institut des Matériaux, Université de Cergy-Pontoise, 5 mail Gay Lussac, Neuville sur Oise, F-95031 Cergy Cedex, France

[#]IEMN, UMR-8520, Université de Valenciennes, Le Mont Houy F-59313 Valenciennes cedex 9, France

ABSTRACT: Recent progress in the field of microsystems on flexible substrates raises the need for alternatives to the stiffness of classical actuation technologies. This paper reports a top-down process to microfabricate soft conducting polymer actuators on substrates on which they ultimately operate. The bending microactuators were fabricated by sequentially stacking layers using a layer polymerization by layer polymerization of conducting polymer electrodes and a solid polymer electrolyte. Standalone microbeams thinner than 10 μm were fabricated on SU-8 substrates associated with a bottom gold electrical contact. The operation of microactuators was demonstrated in air and at low voltage ($\pm 4\text{ V}$).

KEYWORDS: *semi-IPN, conducting polymer, microactuator, flexible substrate, electrochemical microdevices*

Electronic conducting polymers (ECPs) are promising candidates for the development of artificial muscles. When immersed in an electrolytic solution, these materials can convert low voltage stimulations into volume or shape changes through redox reactions.^{1,2} E. Smela et al. demonstrated the potential of these actuators using microfabrication 20 years ago.³⁻⁵ These microactuators operated only in a liquid electrolyte and could suffer from delamination problems.

To operate outside an electrolyte, two ECP electrodes are usually synthesized simultaneously on both faces of membrane, a so-called solid polymer electrolyte (SPE) which acts as an "ion reservoir" (Figure 1A).⁶ Under low applied voltage, inverse volume variation occurs in both electrodes and leads to reversible bending deformations. The delamination issues were then overcome using either a commercial porous or synthesized membranes as SPE.⁷ Despite this progress, the fabrication of open-air actuation devices was only recently demonstrated on a microscale.⁸⁻¹¹ However, their fabrication process was directly inspired by their macroscopic equivalent. Manual handling is required, which limits further scaling down (less than 10 μm thick) and makes it difficult and time-consuming to create many devices in parallel.

Other possible manufacturing methods such as layer-by-layer casting or inkjet printing, nowadays used in organic electronics, are not suitable for ECP microactuators since they require the use of soluble materials or a colloidal dispersion. Although the best candidates for ECP-based actuators (polypyrrole (PPy) and poly(3,4-ethylenedioxythiophene) (PEDOT)) are not normally soluble in any solvent, their soluble or colloidal

dispersion versions (PPy-(2-ethylhexyl)sulfosuccinate PPy-DEHS, PEDOT-polystyrenesulfonic acid PEDOT-PSS) do not attain the same level of performance.

A global rethink of the fabrication process is therefore required to achieve the real integration of ECP-based microactuators and allow further development in micro-robotics, for example.

To achieve this goal, we report on a new and versatile method of synthesis that is fully compatible with microsystems technologies, to design and operate ECP micromuscles in open air on a soft substrate (Figure 1B). The ECP/SPE/ECP trilayers were first obtained by successively polymerizing layers on top of each other, followed by a final intralayer cross-linking and interlayer cobonding (Figure 2A). The first and last layers were obtained using vapor phase polymerization (VPP) of 3,4-ethylenedioxythiophene (EDOT) and the intermediate SPE layer was synthesized as a semi-interpenetrating polymer network (semi-IPN) combining a poly(ethylene oxide) PEO network as the SPE and nitrile butadiene rubber (NBR) for mechanical strength.^{12,13} The additional subtlety of the process derives from the presence of methacrylate cross-linkers in each synthesized layer allowing the final cobonding and preventing de facto any delamination issues. Finally, the compatibility of these novel electroactive materials with conventional micro-patterning methods will be demonstrated. Furthermore, the

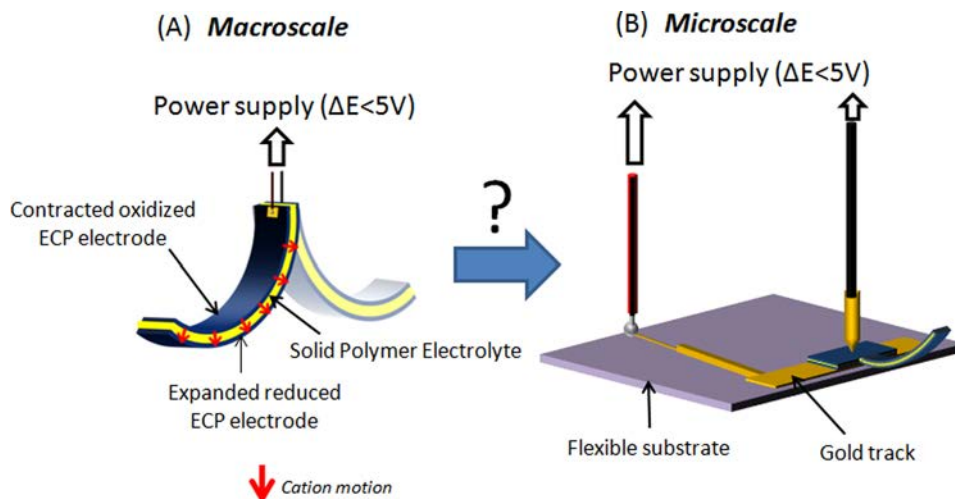


Figure 1. (A) Working principle of open-air macroscopic artificial muscles based on conducting polymers. (B) General structure of the integrated micromuscles on flexible substrate.

process allowed direct integration of electrical connections for the first time, leading to the direct operation of microactuators on flexible substrates.

The first thin layer of ECP is described in detail below because of the specific chemistry used and its importance in the final structure. Active research is currently underway on the synthesis of ECP layers using VPP, in particular to obtain highly conductive layers.^{14–16} However, no work has yet been reported on the use of polar monomers as additives in the synthesis of such ECP layers. The presence of polyethylene glycol methacrylate derivatives (MPEG) is a key element here because these will act as PEO network precursors to ensure adhesion between the layers of the final micromuscles. VPP of EDOT was therefore studied first. It was performed by means of direct chemical oxidation using the commercially available Baytron C Iron(III) tosylate $\text{Fe}(\text{Tos})_3$ solution (40% by weight in butanol), because this oxidant is known to produce highly conducting PEDOT films.¹⁶ To this solution was added 10 wt % poly(ethylene glycol)methyl ether methacrylate (PEGM) (5%) and poly(ethylene glycol)dimethacrylate (PEGDM) (5%) as a monomer and cross-linker, respectively. The oxidant mixture was spin-coated on a poly(vinyl alcohol) (PVA)-coated silicon substrate, which was then placed in a gas-phase polymerization chamber together with a vessel containing EDOT (see Figure S1). The polymerization chamber was then sealed in a vacuum at 40 °C to speed up the process. After this EDOT vapor phase polymerization step, PEDOT-MPEG layers, i.e., PEDOT electrodes containing PEG-based monomers were obtained. The MPEG can therefore be either (i) directly rinsed with methanol, (ii) polymerized by free-radical polymerization before the washing step, leading to PEDOT-PEO composite electrodes, or (iii) left as it is in the PEDOT for subsequent trilayer fabrication.

When MPEG was rinsed directly, the electrical conductivity of the PEDOT layer was measured in order to assess the quality of the electrodes (Figure 2C). The conductivity showed a maximum of around 400 S cm^{-1} for EDOT VPP times shorter than 60 min, and then decreasing gradually to 100 S cm^{-1} as the polymerization time increased to 150 min. Indeed, a longer polymerization time may result in higher structural disorder in the polymer. This eventually leads to a 3D conduction pathway that reduces charge transport and results in higher resistance on

the upper polymer surface, as observed in the case of PEDOT.¹⁷ Concomitantly, PEDOT film thicknesses increased from 0.64 to 1.1 μm (Figure 2D).

Interestingly, although a conductivity of 391 S cm^{-1} was obtained for 30 min of polymerization in the presence of 10 wt % MPEG, it only reached 22 S cm^{-1} for a PEDOT layer synthesized without MPEG (see Figure S2). This result can be explained by recent work showing that the addition of a glycol-based surfactant to the $\text{Fe}(\text{Tos})_3$ solution has a positive effect on the synthesis of highly conducting PEDOT.^{18,19} Indeed, the use of such glycol-based surfactant/oxidant media reduces the number of defects along the conjugated backbone of the polymer by suppressing $\text{Fe}(\text{Tos})_3$ oxidant crystallization, as well as controlling the polymerization rate.

The influence of in situ free radical polymerization of MPEG on the resulting PEDOT layer was also characterized. For that purpose, a free radical initiator was introduced into the oxidant solution with the MPEG before EDOT VPP. The selected initiator was dicyclohexylperoxydicarbonate (DCPD) (3 wt % vs. MPEG). After EDOT VPP times of 30 and 120 min, MPEG was polymerized at 50 °C for 4 h and then for 2 h at 80 °C, leading to an interpenetrated PEO network within the PEDOT film. Polymerization of MPEG resulted in so-called PEDOT-PEO electrodes that were thicker than the corresponding PEDOT without MPEG (Table 1). However, the polymerization of MPEG also led to a significant decrease in electronic conductivity, i.e., from 391 without polymerization to 75 S cm^{-1} after polymerization for the PEDOT layer obtained after 30 min of EDOT VPP. The sample obtained after 120 min VPP polymerization displayed the same behavior (from 192 to 51 S cm^{-1}) (Table 1). This negative effect can be explained by the loosening of the PEDOT packing by the cross-linked PEO polymer,²⁰ but can also be related to the partial degradation of PEDOT during polymerization. Indeed, previous studies have shown that oxygen radicals can induce PEDOT degradation.²¹ In this study, MPEG free radical copolymerization involved homolytic decomposition of the DCPD initiator to produce alkoxy radicals. Oxygen radicals can thus react with PEDOT leading to the partial rupture of the conjugation in the backbone, hence the loss of electroactivity even though it remains relatively high and sufficient for actuator implementation.

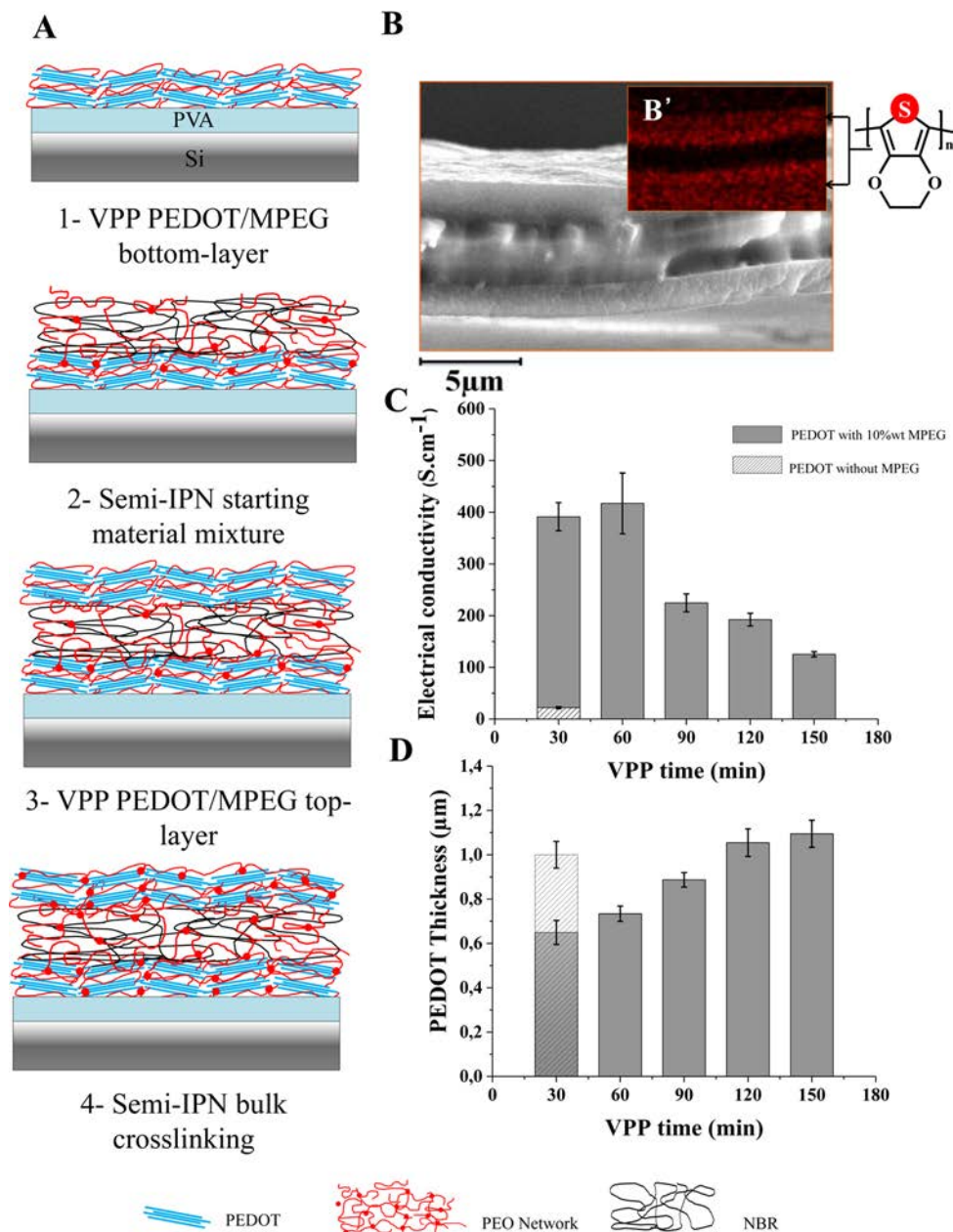


Figure 2. (A) On-substrate fabrication process of the PEO-NBR-PEDOT conducting semi-IPN. (B) SEM image of nonswollen trilayer structure and (B') corresponding EDS picture with sulfur atom cartography (red). (C) Influences of polymerization time on electrical conductivity and (D) on film thickness of PEDOT film synthesized in the presence of 10 wt % of MPEG.

Table 1. Influence of MPEG Free Radical Copolymerization on PEDOT Properties

material	VPP time (min)	thickness (μm)		electrical conductivity (S cm^{-1})	
		MPEG washing*	MPEG polymerization	MPEG washing*	MPEG polymerization
PEDOT-PEO (10%)	30	0.65	1	391	75
PEDOT-PEO (10%)	120	1.1	2.2	192	51

*Washing with methanol leads to the extraction of MPEG from the PEDOT film.

Next, the complete trilayer structure can be synthesized directly on the substrate. The solid polymer electrolyte layer, which will subsequently act as an “ion reservoir” for the device, was then deposited on top of a PEDOT layer containing nonpolymerized MPEG monomers. The solid polymer electrolyte is based on a semi-IPN architecture (Figure 2A) and combines the ion transport properties of a PEO network and

the mechanical properties of a linear NBR. The PEO/NBR 50/50 (w/w) semi-IPN was obtained as described in the experimental section and elsewhere.¹¹ Briefly, all the semi-IPN precursors, i.e., MPEG and NBR, as well as the free radical initiator DCPD, were solubilized in cyclohexanone, a high boiling point solvent. The reactive mixture was spin-coated on the bottom PEDOT-MPEG layer. The two layers were then

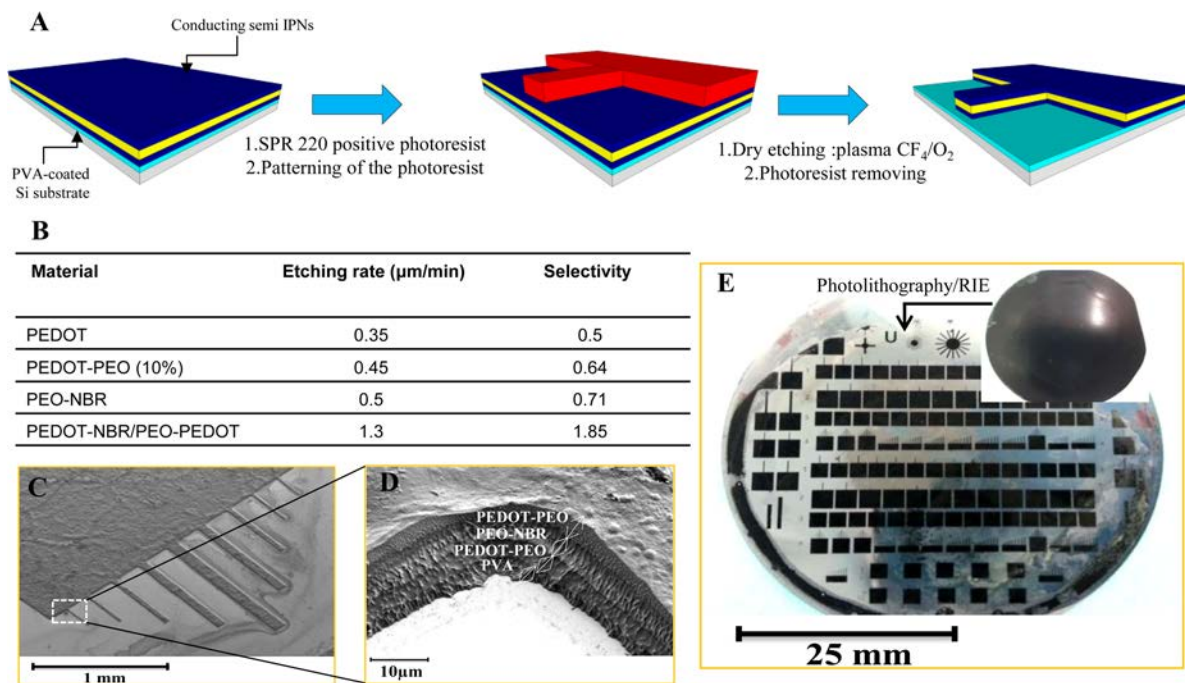


Figure 3. (A) Dry etching process of trilayer actuators on silicon substrate. (B) Etching rates and selectivity of PEDOT, PEDOT-PEO, PEO-NBR semi IPN, and PEDOT-PEO-NBR conducting semi IPNs in plasma of 90/10 O_2/CF_4 at 300 W and 200 mTorr. (C) SEM image of trilayer microstructures and (D) the corresponding zoom-in SEM image. (E) Image of the trilayer microstructures on PVA-coated 2 in. Si substrate. The inset show the trilayer coated substrate before microfabrication.

preprocessed in a vacuum at 50 °C for 45 min to initiate the formation of the PEO network present in each layer and to ensure good mutual adhesion by the polymerizing monomers at the interface. However, complete conversion of methacrylate functions must be avoided to allow the final covalent linking between the semi-IPN layer and the next PEDOT layer (see Figure S4). Finally, the second VPP PEDOT-MPEG layer can be synthesized on the bilayer in the same way as the first conducting layer. Annealing for 4 h at 50 °C and 2 h at 80 °C in a vacuum was carried out to polymerize the methacrylate within the layers but also at the interfaces. The cobonded trilayer was then washed several times in 1-Butanol. The trilayer morphology of the resulting structure was confirmed by scanning electron microscopy (Figure 2B). Energy-dispersive X-ray spectroscopy (EDS) mapping was used to distinguish the sulfur content in PEDOT and shows that the conducting PEDOT-PEO electrodes and PEO-NBR semi-IPN electrolyte layers are connected seamlessly, thereby facilitating intra- and interlayer ion transport, which is essential for the correct operation of an electrochemical device.

Conventional microfabrication techniques were then used to design trilayer in parallel devices. Material patterning was performed by means of photolithography and reactive ion etching (RIE) (Figure 3A). The positive photoresist SPR220-7 μm was spin-coated to be used as an etching mask. Dry etching was then performed using RIE (more details are available in the Supporting Information).^{9,11} A high etch rate ($1.3 \mu\text{m min}^{-1}$) and good selectivity (1.85) were obtained using the 90/10 O_2/CF_4 gas ratio (Figure 3B). In these conditions, as illustrated in Figure 3C, D, microfabrication of trilayer microstructures can be performed with precise control of the geometry, size and shape. The proof of concept presented in Figure 3E contains 500 ECP elements with diameters ranging from 500 to 5 μm and lengths from 3000 to 50 μm . In other words, large-scale

batch fabrication of precisely defined ECP-based micro-electrochemical devices can be performed directly on a Si substrate.

The last step in demonstrating actuation of ECP micro-muscles on flexible substrates was to fabricate and pattern such structures, as described earlier, on top of a specifically designed wafer. Figure 4A illustrates the process sequences. Considering that microbeams must be produced in standalone form with integrated electrical contacts, a specific process must be set up. Thus, a locally UV-exposed/cross-linked epoxy-based photoresist SU-8 was chosen as the flexible substrate and will act as the fulcrum for microbeam actuators (Figure 4A.2). Base gold electrodes were then patterned on top of the cross-linked SU-8 layer to form stable electrical connections for flexion producing muscles (Figure 4A.3). Because of solubilization of the non-cross-linked SU-8 photoresist during the development of the gold electrodes, a PVA sacrificial layer was used to fill the remaining 90 μm deep cavity (Figure 4A.4). The structure was ready to be coated with a PEDOT/PEO-NBR/PEDOT trilayer and then patterned as described previously (Figure 4A.5, 6 and Figure 4B). Finally, the PVA sacrificial layer was dissolved in water to release the microbeams locally (Figure 4A.7) (more details are available in the Supporting Information). The ions required for the redox process of the conducting polymer electrodes were then incorporated through a swelling step, turning these microstructures into electroactive micromuscles. N,N-ethylmethylimidazolium bis(trifluoromethanesulfonyl)imide (EMITFSI) ionic liquid was chosen as the electrolyte. Standalone electroactive polymer microbeams were then obtained: the base of the device rests on an SU-8 flexible surface with gold electrodes integrated on the base (Figure 4C). A micromechanical gold tip was positioned on top of the trilayer to make the second electrical connection.

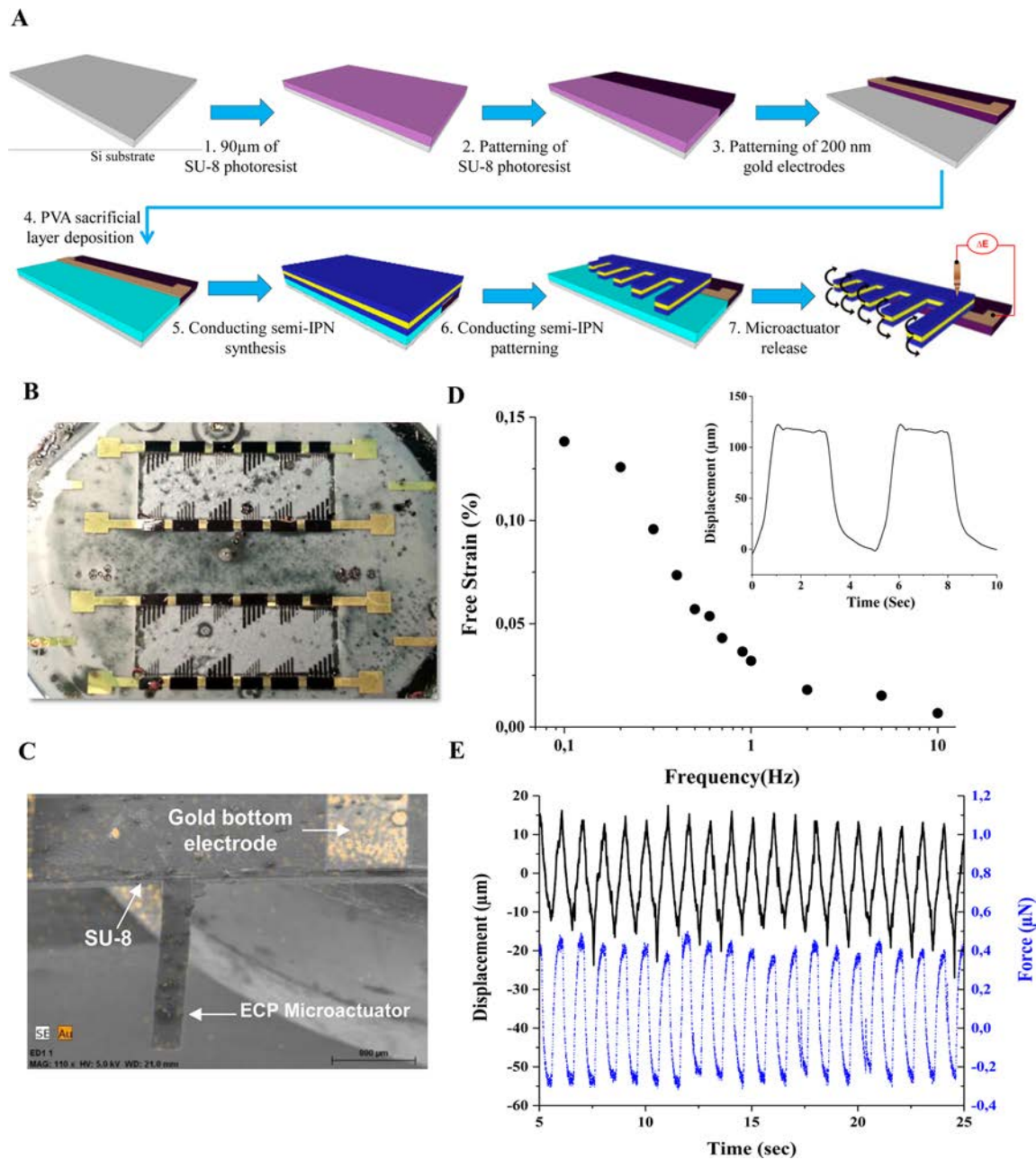


Figure 4. (A) Top-down fabrication process of trilayer microactuators on flexible substrate, (B) images of microactuators after batch microfabrication, (C) standalone microactuator on SU-8 substrate, (D) free strain as a function of frequency of the microactuator (Lwh : $650\ \mu\text{m} \times 100\ \mu\text{m} \times 10\ \mu\text{m}$) under $\pm 4\ \text{V}$ square wave potential, (E) tip displacement and output force versus time at 0.2 Hz.

A demonstration of air-operation of the micromuscles directly on SU-8 is presented. The microdevices were characterized by their maximum performances, i.e., maximum displacement, expressed in terms of free strain, and maximum output force. The free strain as a function of the electrical stimulation frequency under $\pm 4.0\ \text{V}$ square wave potential is shown in Figure 4D. Bending toward the anode can be observed during actuation indicating a volume contraction during oxidation. This behavior indicates that cation motion is the main driving mechanism in this material as it has been shown on macro devices.²² Thus, the electrodes switch from an expanded reduced state to a contracted oxidized one. In the low frequency region (0.05–0.2 Hz), the microbeams show a maximal free strain of 0.13%, corresponding to a peak-to-peak displacement of $127\ \mu\text{m} \pm 6\ \mu\text{m}$ for a $650\ \mu\text{m}$ long beam. At

such low frequencies, the two electroactive PEDOT layers are fully oxidized and reduced, leading to maximum charge transfer and then to maximum bending displacement. For frequencies up to 10 Hz, the microactuator showed a linear decrease in mechanical response. This indicates that less and less PEDOT undergoes the redox process and is then involved in the actuation as the frequency increases. Nonetheless, at 1 Hz, the microbeams still present significant mechanical amplitude of 0.03%. Figure 4E shows both the tip displacement and output force as a function of time measured for 20 repeated cycles at 1 Hz. Interestingly, this micromuscle produces a fast mechanical response with a free displacement of $32\ \mu\text{m}$ and a maximum output force of $0.75\ \mu\text{N}$.

To summarize, this work proposes a novel and versatile approach to fabricate, pattern, and operate solid-state electro-

chemical micromuscles directly on flexible surfaces through processes fully compatible with microsystems. The cobonded trilayer structures are fabricated by innovative sequential layer stacking. The two PEDOT electrodes were obtained by vapor phase polymerization and the intermediate SPE layer as a PEO-NBR semi-interpenetrating polymer network. These materials have been successfully patterned using photolithography and RIE techniques and are easily scalable for the simultaneous batch-production of microdevices with hundreds of electro-mechanical structures. We have demonstrated that they can be directly synthesized on an SU-8 flexible substrate with integrated electrical connections. Under low voltage, the resulting microbeams have a strain of up to 0.13% and output forces just under 1 μ N. To the best of our knowledge, this is the first time that electrochemical micromuscles operating in air have been manufactured on a flexible substrate, eliminating risky multistage processing typically reflected in the literature to date. Further studies are still in progress and are focused on the actuation speed and on the size dependence of the actuator responses. These results open up new prospects for the accurate and cost-effective production of fully flexible micro-electromechanical systems. Moreover, such an approach could be easily extended to a more general procedure by varying the choice of functional materials and their synthesis conditions. Indeed, numerous other electrochemical microdevices such as sensors, optoelectrical devices, supercapacitors, or micro-batteries with a trilayer structure could be designed, leading to new prospects for flexible microsystems.

ASSOCIATED CONTENT

Supporting Information

The Supporting Information is available free of charge on the ACS Publications website at DOI: 10.1021/acsami.5b09577.

Description of the material, experimental data about the effect of MPEG on PEDOT electrical conductivity, experimental details about the top-down fabrication of standalone trilayer microactuators, additional scanning electron microscopy images (PDF)

AUTHOR INFORMATION

Corresponding Author

E-mail: eric.cattan@univ-valenciennes.fr.

Notes

The authors declare no competing financial interest.

ACKNOWLEDGMENTS

The authors thank the ANR for its financial support (Grant ANR-09-BLAN-0110) and the European Network on Artificial Muscles (ESNAM). This work was partly supported by the French RENATECH network.

REFERENCES

- (1) Baughman, R. H. Conducting Polymer Artificial Muscle. *Synth. Met.* **1996**, *78* (3), 339–353.
- (2) Smela, E. Conjugated Polymer Actuators for Biomedical Applications. *Adv. Mater.* **2003**, *15* (6), 481–494.
- (3) Smela, E. Microfabrication of PPy Microactuators and other Conjugated Polymer Devices. *J. Micromech. Microeng.* **1999**, *9*, 1–18.
- (4) Jager, E. W. H.; Smela, E.; Inganäs, O.; Lundström, I. Polypyrrole Microactuators. *Synth. Met.* **1999**, *102*, 1309–1310.
- (5) Jager, E. W.; Smela, E.; Inganäs, O. Microfabricating Conjugated Polymer Actuators. *Science* **2000**, *290* (5496), 1540–1545.

- (6) Otero, T. F.; Cortes, M. T. Artificial Muscles with Tactile Sensitivity. *Adv. Mater.* **2003**, *15*, 279–282.
- (7) Wu, Y.; Alici, G.; Spinks, G. M.; Wallace, G. G. Fast Trilayer Polypyrrole Bending Actuators for High Speed Applications. *Synth. Met.* **2006**, *156* (16–17), 1017–1022.
- (8) Alici, G.; Devaud, V.; Renaud, P.; Spinks, G. Conducting Polymer Microactuators Operating in Air. *J. Micromech. Microeng.* **2009**, *19* (2), 025017.
- (9) Khaldi, A.; Plesse, C.; Soyer, C.; Cattan, E.; Vidal, F.; Legrand, C.; Teyssié, D. Conducting Interpenetrating Polymer Network Sized to Fabricate Microactuators. *Appl. Phys. Lett.* **2011**, *98* (16), 164101.
- (10) Gaihe, B.; Alici, G.; Spinks, G. M.; Cairney, J. M. Synthesis and Performance Evaluation of Thin Film PPy-PVDF Multilayer Electroactive Polymer Actuators. *Sens. Actuators, A* **2011**, *165* (2), 321–328.
- (11) Maziz, A.; Plesse, C.; Soyer, C.; Chevrot, C.; Teyssié, D.; Cattan, E.; Vidal, F. Demonstrating kHz Frequency Actuation for Conducting Polymer Microactuators. *Adv. Funct. Mater.* **2014**, *24*, 4851–4859.
- (12) Klemmner, D.; Sperling, L. H.; Utracki, L. A. *Interpenetrating Polymer Networks*; American Chemical Society: Washington, D.C., 1994.
- (13) Vidal, F.; Plesse, C.; Teyssié, D.; Chevrot, C. Long-Life Air Working Conducting Semi-IPN/Ionic Liquid Based Actuator. *Synth. Met.* **2004**, *142* (1–3), 287–291.
- (14) Winther-Jensen, B.; Chen, J.; West, K.; Wallace, G. Vapor Phase Polymerization of Pyrrole And Thiophene using Iron(III) Sulfonates as Oxidizing Agents. *Macromolecules* **2004**, *37*, 5930–5935.
- (15) Winther-Jensen, B.; Breiby, D. W.; West, K. Base Inhibited Oxidative Polymerization of 3,4-ethylenedioxythiophene with Iron(III) Tosylate. *Synth. Met.* **2005**, *152* (1–3), 1–4.
- (16) Fabretto, M. V.; Evans, D. R.; Mueller, M.; Zuber, K.; Hojati-Talemi, P.; Short, R. D.; Wallace, G. G.; Murphy, P. J. Polymeric Material with Metal-Like Conductivity for Next Generation Organic Electronic Devices. *Chem. Mater.* **2012**, *24*, 3998–4003.
- (17) Ugur, A.; Katmis, F.; Li, M.; Wu, L.; Zhu, Y.; Varanasi, K. K.; Gleason, K. K. Low-Dimensional Conduction Mechanisms in Highly Conductive and Transparent Conjugated Polymers. *Adv. Mater.* **2015**, *27* (31), 4604–4610.
- (18) Zuber, K.; Fabretto, M.; Hall, C.; Murphy, P. Improved PEDOT Conductivity via Suppression of Crystallite Formation in Fe(III)-Tosylate During Vapor Phase Polymerization. *Macromol. Rapid Commun.* **2008**, *29* (18), 1503–1508.
- (19) Fabretto, M.; Jariego-Moncunill, C.; Autere, J. P.; Michelmoré, A.; Short, R. D.; Murphy, P. High Conductivity PEDOT Resulting from Glycol/Oxidant Complex and Glycol/Polymer Intercalation during Vacuum Vapour Phase Polymerisation. *Polymer* **2011**, *52* (8), 1725–1730.
- (20) Shaplov, A. S.; Ponkratov, D. O.; Aubert, P. H.; Lozinskaya, E. I.; Plesse, C.; Maziz, A.; Vlasov, P. S.; Vidal, F.; Vygodskii, Y. S. Truly Solid State Electrochromic Devices Constructed from Polymeric Ionic Liquids as Solid Electrolytes and Electrodes Formulated by Vapor Phase Polymerization of 3,4-ethylenedioxythiophene. *Polymer* **2014**, *55* (16), 3385–3396.
- (21) Verge, P.; Vidal, F.; Aubert, P.-H.; Beouch, L.; Tran-Van, F.; Goubard, F.; Teyssié, D.; Chevrot, C. Thermal Ageing of Poly(ethylene oxide)/Poly(3,4-ethylenedioxythiophene) Semi-IPNs. *Eur. Polym. J.* **2008**, *44* (11), 3864–3870.
- (22) Festin, N.; Maziz, A.; Plesse, C.; Teyssié, D.; Chevrot, C.; Vidal, F. Robust Solid Polymer Electrolyte for Conducting IPN Actuators. *Smart Mater. Struct.* **2013**, *22* (10), 104005.